

GEM-based detectors for direct detection of low-mass WIMP, solar axions and narrow resonances (quarks).

B.M.Ovchinnikov, V.V.Parusov*

Institute of Nuclear Research of Russian Academy of Sciences, Moscow.

*Corresponding author; e-mail: parusov@inr.ru

Abstract

Gas electron multipliers (GEMs) with wire (WGEMs) or metal electrodes (MGEMs), which don't use any plastic insulators between electrodes are created. The chambers containing MGEMs (WGEMs) with pin-anodes are proposed as detectors for searching of spin-dependent interactions between Dark Matter (DM) particles and gases with nonzero-spin nuclei (^1H , D_2 , ^3He , ^{19}F , ^{21}Ne , ^{129}Xe , ^{131}Xe , etc.). In this paper, we present a review of such chambers. As photosensitive addition we use of H_2 , C_2H_4 , CF_4 , TMAE, etc.

For investigation of the gas mixtures $\text{Ne}+10\%\text{H}_2$, $\text{H}_2(\text{D}_2)+3\text{ppmTMAE}$, the chamber containing WGEM with pin-anodes detection system was constructed. In this paper we present the results of an experimental study of these gaseous mixtures excited by an α - source. Mixture of $\text{Ar}+40\text{ ppm C}_2\text{H}_4$ and mixture $50\%\text{Xe}+50\%\text{CF}_4$ have been investigated. The spatial distributions of photoelectron clouds produced by primary scintillations on α - and β -particle tracks, as well as the distributions of photoelectron clouds due to photons from avalanches at the pin-anode, have been measured for the first time.

In our experiments as another filling of the chambers for search of low-mass WIMP ($<10\text{ GeV}/c^2$), solar neutrino and solar axions with spin-dependent interaction we propose to use the mixtures: $\text{D}_2+3\text{ppmTMAE}$, $^3\text{He}+3\%\text{CH}_4$, $^{21}\text{Ne}+10\%\text{H}_2$, at pressure 10-17 bar. And in our experiment with liquid mixtures is used the mixtures with ^{19}F ($\text{LXe}+\text{CF}_4$) and mixture with ^1H ($\text{LCH}_4+40\text{ppm TMAE}$).

The time projection chamber (TPC) with the mixture $\text{D}_2+3\text{ppmTMAE}$ filling at a pressure 10 bar allow to search of spin-dependent interactions of solar axions and deuterium (section 8). As well as we present the detecting systems for search of narrow pp-resonances (quarks) in accelerators experiments (section 9).

Finally, we discuss principles of operation of GEMs with pin-anodes as well as plans for constructing of large scale (150 mm x 150 mm) MGEM detectors.

Keywords: MGEM, pin-anodes, Low-Mass WIMP, Axions, Quarks, TPC, SD-interactions, H_2 , CF_4 , CH_4 , TMAE.

1. Introduction

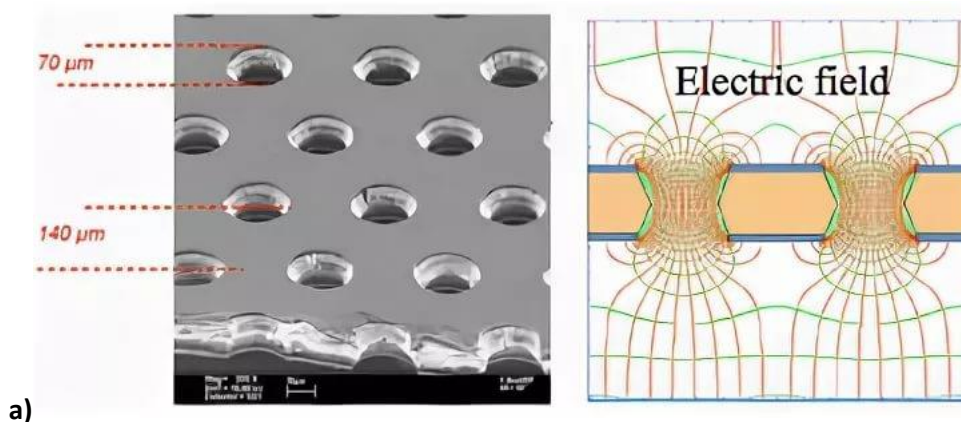
More than forty years ago G. Charpak and F. Sauli have introduced their Multi-Step Chambers to overcome limitations of gain in Parallel-Plate and Multi-Wire Proportional Chambers (MWPC) [1, 2]. These MWPCs have revolutionized detection systems in high energy physics.

Currently there are different types of detectors for fast detection and localization of charged particles exist. One of them is a Gas Electron Multiplier (GEM). A standard Gas Electron Multiplier [2,3,4] consists of a thin composite sheet (plate) with two metal layers separated by a thin insulator and pierced by a regular matrix of open channels. These plates contain through holes on all their area, separation distances and diameters of which are approximately equal to the plate thickness (Fig.1a). Inside these holes, which are filled with corresponding gases, in presence of strong electric fields, a multiplication of electrons takes place. GEMs provide the best spatial resolution and higher rate than the wire chambers (MWPC). More coarse macro-patterned detectors are thick-GEMs (THGEM) [5, 6, 7] or patterned resistive thick GEM devices (RETGEM) [8].

However, the most essential disadvantage of GEMs consists in their low reliability and stability. The matter is that in a process of dispersion of the GEM's cathode electrodes by positive ions of proportional avalanches in GEM with metal or high-resistive electrodes (RETGEM). The sedimentation of the sprayed carrying-out material on the walls of holes with subsequent leaks and breakdowns between electrodes takes place. It leads to subsequent decrease of the potential difference between GEM's electrodes and corresponding reduction of the multiplication factor in an avalanche (Fig.1b).

Micro-pattern gaseous detectors (MPGD), due to their tiny electrode structure and small avalanche gaps (Fig.1c), are very fragile and can be easily damaged by sparks appearing at high operational gains (typically at gains of 10^4 or slightly more) [7].

Therefore, we were concentrated on development of more robust designs of GEM detectors with wire (WGEM) or metal electrodes (MGEM). The idea of WGEM without plastic insulators was first mentioned in our work [9-12]. In our subsequent works [13] a MGEM with metal electrodes of diameter of 22 mm was designed and tested. In the paper [14] we have described a novel concept of MGEMs.]. In our next works [15-18, 21, 25] it was suggested that the search for spin-dependent WIMP-nucleon interactions with help of detecting system GEM + pin-anodes can be performed.



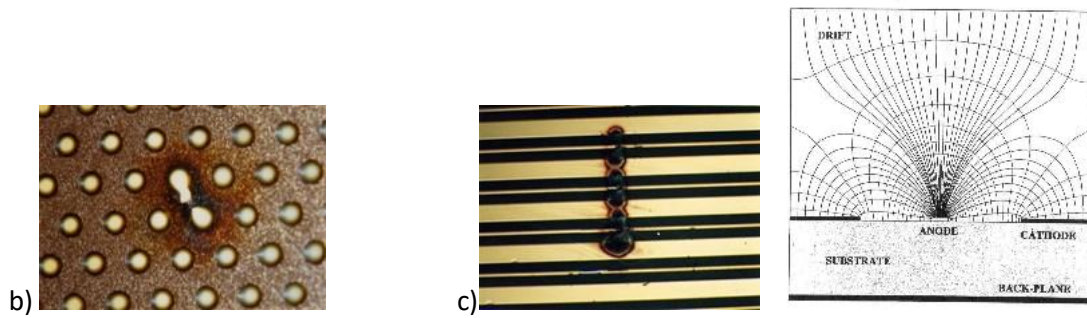


Fig.1. **a)** Gas Electrons Multiplier (GEM), **b)** Resistive thick GEM (RETGEM), **c)** Micro-pattern gaseous detectors (MPGD). The sedimentation of the sprayed carrying-out material on the walls of holes (insulators) with subsequent leaks and breakdowns between electrodes takes place (b, c).

2. GEMs with wire electrodes (WGEM)

In our works [9-12] WGEMs with wire electrodes and no plastic insulators between them were created. The WGEMs [9] used macroscopic windows of size 1 mm by 1 mm, while WGEMs [10-12] used windows of size 0,5 mm by 0,5 mm. The gap between the wire electrodes was equal to 1 mm. The design of wire GEMs and the results of their tests are shown in Fig.2 and Fig.3.

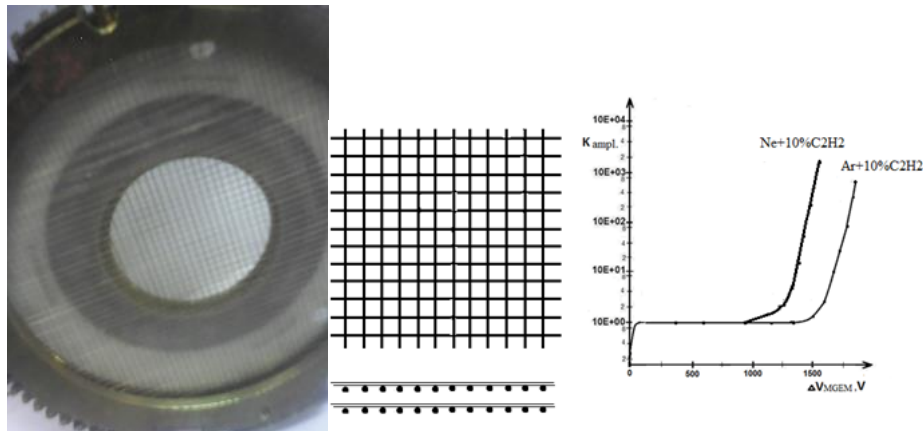


Fig.2. Design of WGEMs and results of their tests [9].

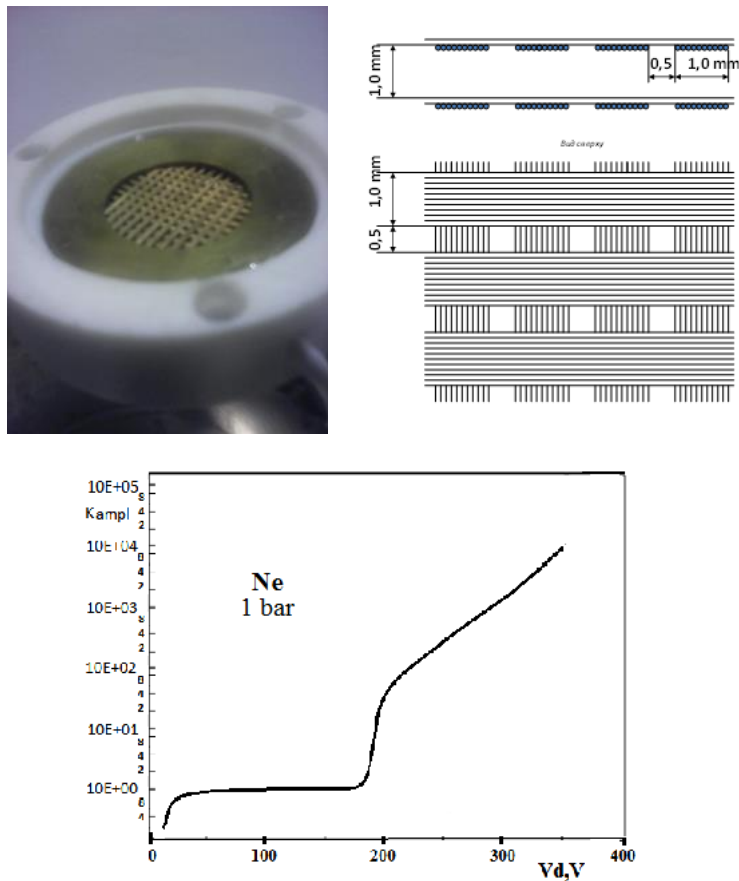


Fig.3. Design of WGEMs and results of their tests [10-12].

3. GEM with metal electrodes (MGEM)

In the work [12] a MGEM with metal electrodes and sensitive area of 22 mm by 22 mm for the first time was demonstrated. The electrodes were made by drilling of 1 mm holes with a step between them of 1.5 mm in to 1 mm thick brass plates (see Fig.4). One disadvantage of that MGEM [13] is large duration of the process of drilling the holes in the electrodes, especially for a case of small diameters and small steps between holes. In addition to that, formation of agnails at the edges of holes in a process of drilling is possible. Another problem of drilling of holes with drilling machines consists in difficulty of production of large area MGEM electrodes with high accuracy of sizes of holes and their positions on various plates.

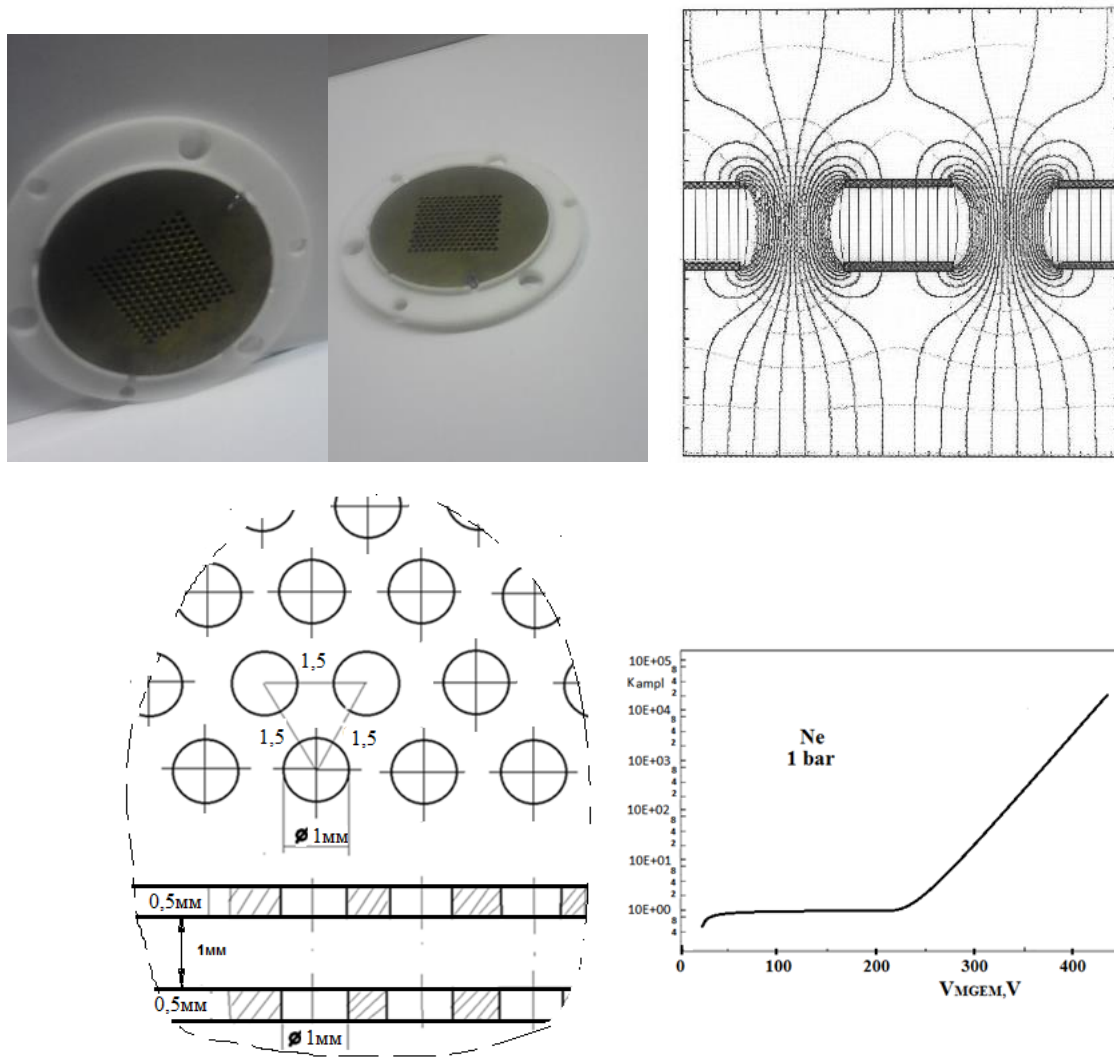


Fig.4. Design of metal GEM, electric field and results of tests [13].

4. MGEM with the etching of holes

In the work [14] the gas electron multiplier with metal electrodes (MGEM), differing by its simplicity, high precision and technological effectiveness in production, as well as reliability and stability of its operation, is made and tested. To eliminate certain specific shortcomings (see Introduction), in this work metal electrodes were made by a method of drawing a mask on 0.3 mm thick brass plates with 0.3 mm diameter holes and 0.5 mm step between them (fig.5) with subsequent double-side etching of the holes.

As far as the initial brass plate was cut from 0.3 mm thick rolled foil, the produced electrodes had a curved shape. Therefore, at assembling, between the MGEM electrodes a fluoroplastic spacer was introduced to increase resistance on the pass of leakage charges between the electrodes. From the outer sides both electrodes were pressed to fluoroplastic plate by additional steel rings of 2 mm thickness.

By means of central 4 mm holes in electrodes and special insulating bolts, the GEM electrodes were mutually positioned in such a way that the relative displacements of holes didn't exceed 0.02 mm. The gap between electrodes was chosen to be equal to 1 mm. In this design a sensitive area GEM with holes had a diameter of $D=75$ mm. The GEM was tested in the chamber (Fig.6.) with various filling gases: Ar +10% C_2H_4 (1 and 0.4 bar), Ne +(($O_2 + N_2 + H_2O$)· 10^{-6})(1 and 0.4 bar), Ar +10% CH_4 (1 bar).

The results of tests at irradiation of the drift gap of the chamber by alpha-particles (Pu^{239}) are presented in Fig.5. It is visible, that Ne provides the maximum coefficient of multiplication at the smallest potential difference between electrodes before the breakdown happens.

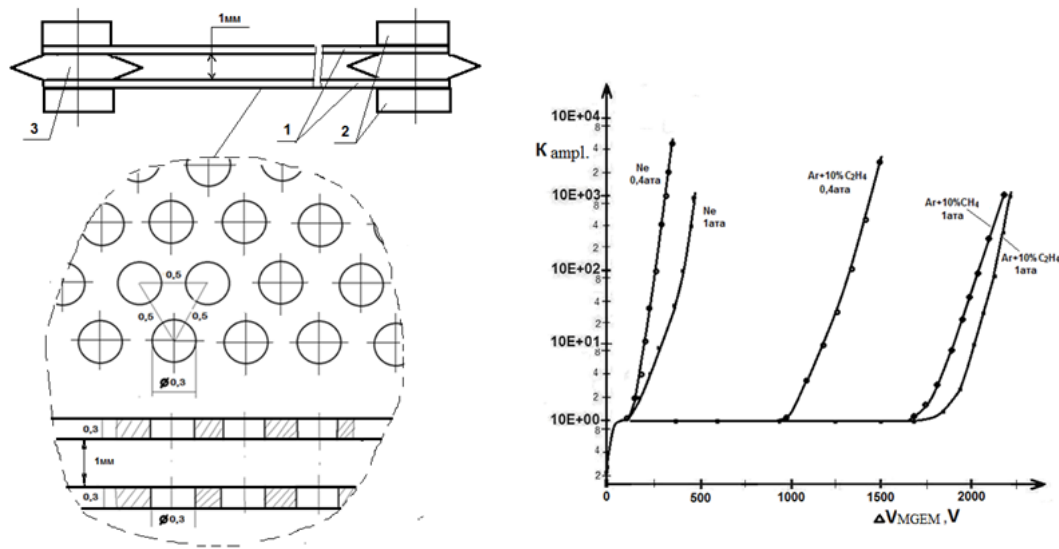


Fig.5. Left: design of MGEM: 1-plates of MGEM, 2-clamping rings, 3-layer from fluoroplastic. Right: amplification of MGEM filled with different gases.



Fig.6. Chamber for test MGEM.

5. The detecting chambers with system GEM + pin-anodes for direct detection of WIMP.

In work [15] the idea of focusing screen with holes + system pin-anodes already was shown (section 5.1). The wire gas electron multipliers in combination with pin-anodes are proposed for detection of events:

- (1) In the gas phase of a double-phase argon chamber (section 5.2);
- (2) In chamber for direct detection of WIMP with mass $\leq 0.5 \text{ GeV}/c^2$ (section 5.4);
- (3) In chamber with gas mixture $\text{H}_2(\text{D}_2) + 3\text{ppm TMAE}$ for direct detection of WIMP with mass $\leq 10 \text{ GeV}/c^2$ and solar axions (section 5.5);
- (4) In double-phase chambers with $\text{LXe} + \text{CF}_4$ and $\text{LCH}_4 + \text{TMAE}$ filling (section 7).
- (5) And, in scintillation and ionization fast chambers with mixture $\text{Xe} + \text{CF}_4$ for accelerators experiments (section 9).

In the time projection chamber (TPC) with the mixture $\text{D}_2 + 3\text{ppmTMAE}$ filling we use of two-step system GEM + MWPC (section 8).

5.1 A liquid-methane ionization chamber

A liquid-methane ionization chamber with a system of focusing screen + pin-anodes is proposed as a setup to search for spin-dependent interactions of DM particles [15]. The anode of the chamber is placed in gaseous methane above liquid methane. The anode consists of a system of pins. The Focusing screen is placed between the Anode and liquid methane. The screen has a system of holes concentrically on the relevant pin-anode. The values of electrical potentials on the electrodes of the chamber are set in such a way that all electrical lines of force are focused on the pin-anodes. We provide only the idea of using a specially designed liquid-methane ionization chamber in an experiment aimed at searching for the (mostly) low mass DM based on their spin-dependent interactions (see section 7.2).

5.2 Double-phase argon chamber

Multichannel WGEM + system pin-anodes are proposed for detection of events in the gas phase of a double-phase argon chamber [16, 17]. Hydrogen with a concentration of 10 % is added to argon to eliminate feedbacks via photons emitted by excited argon molecules in avalanche development processes during detection of events in the gaseous argon. A maximum electron multiplication coefficient of ~ 300 has been obtained for the multichannel wire gas electron multipliers with a 1 mm gap used to detect α -particles in the $\text{Ar} + 10\% \text{H}_2$ mixture at a pressure of 1 bar. When a pin anode is used, the maximum electron multiplication factor for α -particles is $\sim 2.5 \times 10^5$. It has been experimentally shown that adding H_2 with a concentration of 100 ppm to liquid argon has no effect on the singlet component of the scintillation signal in the liquid argon and reduces the emission efficiency relative to the pure argon gas phase only slightly (by 20%).

5.3. A method for background reduction in experiments for direct detection of WIMPs.

To suppress the β , γ and n_0 backgrounds, we proposed [18] a addition in liquid argon of photosensitive dopants and a comparison of scintillation (S1) and ionization signals (S2) for every event is suggested. The addition in liquid Ar of photosensitive TMA, TMG or C₂H₄ [19] and suppression of triplet component of scintillation signals ensures the detection of scintillation signals with high efficiency and provides a complete suppression of the electron background.

In work [20] we investigated of scintillation (S1) and ionization signals (S2) on a mixture of Ar + 40ppm C₂H₄ at a pressure of 5 bar.

The measurements were taken inside the chamber similar a chamber with pin-anode (see Fig. 5 left). The mixture was irradiated with α (239Pu) and β (63Ni) particles. The chamber was used with potentials of pin-anode $V_a = 1300$ V, $K_{amp} \sim 10^4$ (β) and $V_a = 520$ V, $K_{amp} = 30$ (α).

Peak S1 is associated with the cloud of photoelectrons from the chamber volume due to scintillation photons with $\lambda = 128$ nm, which are emitted upon excitation of argon atoms with $\alpha(\beta)$ particles: $h\nu + C_2H_4 \rightarrow C_2H_4^* + e^-$. Peak S2 is due to ionization electrons from $\alpha(\beta)$ particles (Fig. 5). Peak S3 fluctuates in the amplitude for different events, since the β -particle spectrum lies in the range of $E^{min} - E^{max}$ (17 - 67 KeV). Peak S3 can be attributed to the cloud of photoelectrons from the chamber volume produced by photons from avalanches at the pin-anode.

The results obtained in our study suggest that it is possible to develop large volume detectors capable of detecting scintillations with a 100% geometrical efficiency, by contrast to the well known detection techniques based on photomultipliers having efficiency of only a few percent [27].

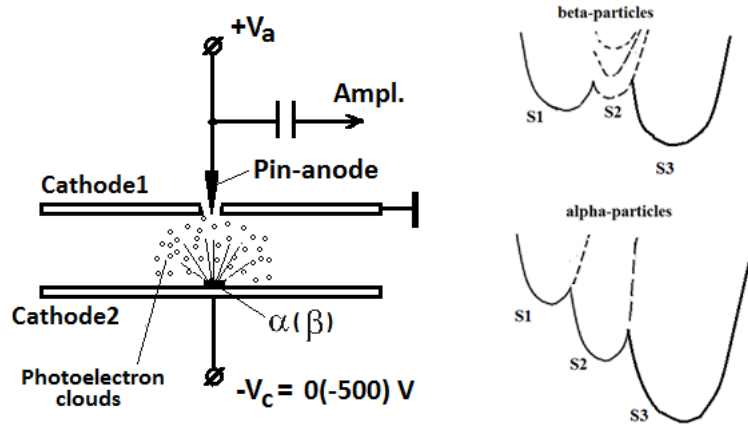


Fig. 5. The chamber filled with the mixture of Ar + 40ppm C₂H₄ at a pressure of 5 bar. The mixture was irradiated with α (239Pu) and β (63Ni) particles. The chamber was used in potentials of pin-anode $V_a = 1300$ V, $K_{amp} \sim 10^4$ (β -particles) and $V_a = 520$ V, $K_{amp} = 30$ (α -particles). $-V_c = 0$ V.

5.4 The chamber for direct detection of WIMP with mass ≤ 0.5 GeV/ c^2 .

The detectors with pure NaI, Xe or Ar [24, 31] make it possible to search WIMPs with large masses (up to dozens or hundreds GeV), as far as the energy of nuclear recoils in these detectors from low mass WIMPs is low. To account for yearly modulation effect in DAMA-LIBRA experiment [28, 29]

J.Va'vra has supposed [31] that this effect is explained by low mass WIMP scattered at protons in H_2O molecules, which is contained in NaI crystals at about 1ppm level (see Table 1.)

The chamber for direct detection of WIMP with mass $\leq 0.5 \text{ GeV}/c^2$ was developed [21]. The chamber (see Fig.7) is filled with gas mixture Ne+10% Hydrogen +0,15ppm TMG. In this chamber for the events detection it was used a system GEM +pin-anodes, which provide the energy threshold about eV. The electron background is suppressed due to photosensitive addition of TMG. For a direct detection of WIMP it is proposed to use a liquid argon chamber with Hydrogen dissolved in liquid argon at a concentration 100ppm+0,015ppm TMG. Based on the work [22], where in a spherical proportional detector the energy threshold is about 100eV, while the amplification factor of the detecting system is about 10^4 , we estimate the threshold of our experiment to be about $\sim 100 \text{ eV} \cdot 10^4 / 5 \cdot 10^7 < 1 \text{ eV}$. The H_2 -filling provides an efficient suppression of the electron background, because of the short track of recoil protons, compared to the one from background electrons [30]. As another filling of the chamber is used the mixture ^{21}Ne +10%deuterium (D2) for search of spin-dependent interaction [23, 35, 36].

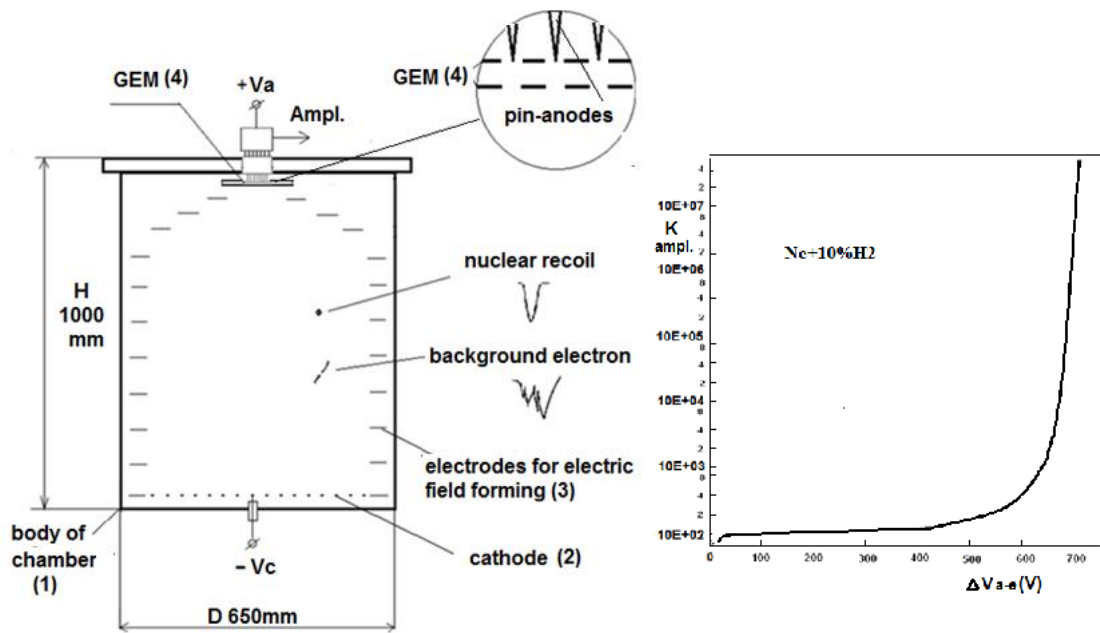


Fig.7. Chamber with a system GEM +pin-anodes and corresponding results of tests of the detection system (Fig.8). Coefficient of electron multiplication as a function of the anode voltage. The chamber is filled with a mixture of Ne+10%H₂ at a pressure of 1 bar is exposed to α particles.

5. The study of system GEM + pin-anode for search for low-mass WIMP and solar axions.

In our work [25] the chamber for direct detection of WIMPs with mass $< 10 \text{ GeV}/c^2$ and axions, emitted from the Sun, was developed. For searching the solar axions is used of mixture D₂ + 3 ppm TMAE in this experiment. The chamber is filled with a gas mixture H₂ +3ppm TMAE (5, 10 bar), or D₂ + 3ppm TMAE (5, 10 bar). These gas fillings allow to suppress the electron background [18]. For detection of events is used a system GEM + pin-anodes (Fig.8) with coefficient multiplication of about 10^5 (see Fig.9) and the chamber of the previous experiment (Fig.7). Collisions of WIMPs with H₂ provide recoil

protons with energies of several keV (see Table 1). An addition of TMAE with a low ionization potential (5,36 eV) provides detection of recoil protons.

As another filling of the chamber is used the mixture deuterium (D_2) + 3ppm TMAE, because:

(1) the energy of D-recoil is two times more than proton recoil.

(2) the spin (J_S) of nuclear deuterium is equal 1 (the spin of nuclear hydrogen is equal $\frac{1}{2}$) [23]. This gives the increase the cross section 3-times as compared with hydrogen. Scattering cross section is $\sigma_{SD} \sim J_S \cdot (J_S + 1)$.

Because the energy of axion is equal to ~ 1 keV [26], it transfers the energy to recoil deuterium. The H_2 -filling provides the electron background suppression, because the recoil protons in H_2 -medium have the short track [30], as distinguished from background electrons.

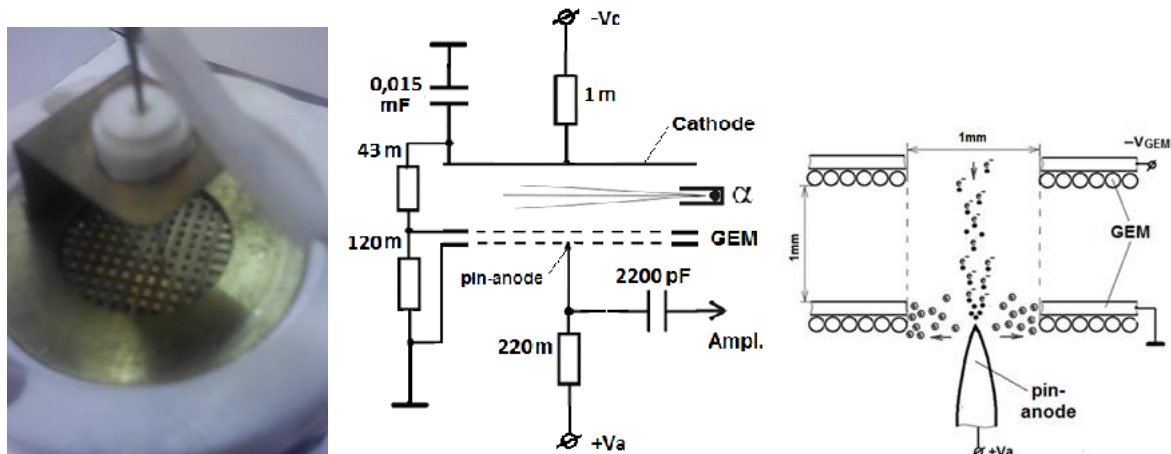


Fig.8. Detection system for testing of WGEM + pin-anode with diagram of the travel of positive ions from avalanches developed at the pin and electrons being collected at the pin.

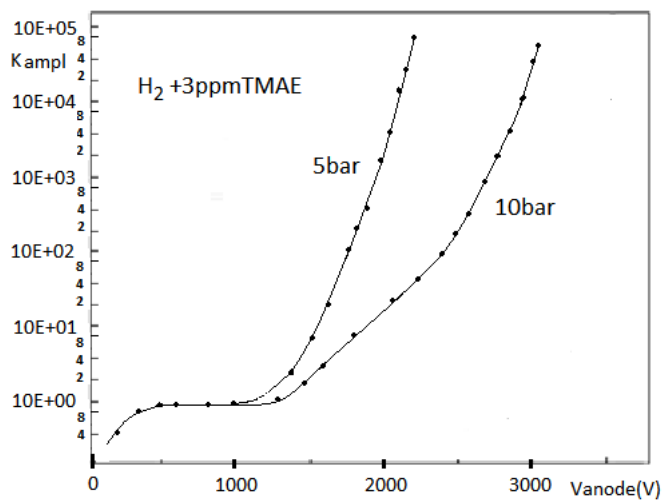


Fig.9. Measured amplification of a system GEM + pin-anode.

a)

WIMP [GeV/c^2]	Nucl.	$E_{nr}(\text{keV})$
0,5	H	1,91
1,0	H	4,30
1,5	H	6,20
2,0	H	7,65
2,5	H	8,78
3,0	H	9,68
0,5	Na	0,19
1,0	Na	0,73
1,5	Na	1,57
4,0	Na	9,07

b)

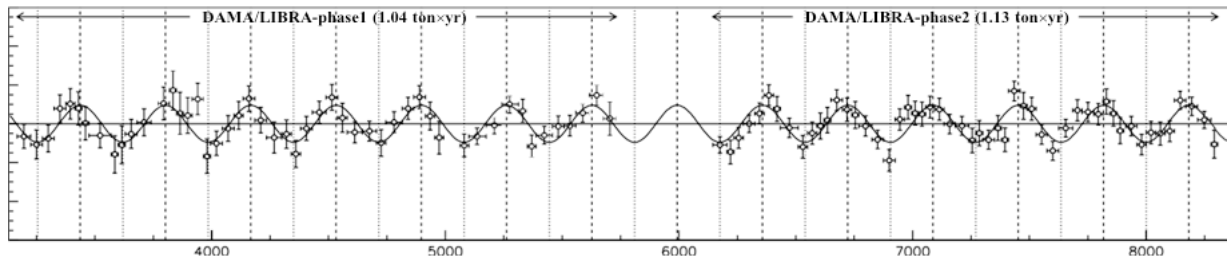


Table1. Maximum calculated nuclear recoil energy $E_{nr}(\text{keV})$ as a function of WIMP mass (GeV/c^2) for two targets: hydrogen and sodium (a). J.Va'vra has supposed [31] that this effect is explained by low mass WIMP scattered at protons in H_2O molecules(H^+), which is contained in NaI crystals at about 1ppm level. Residual rate for single-hit scintillation events in the (2–6) keV energy interval in DAMA/LIBRA–phase1[28] and DAMA/LIBRA–phase [29](b).

6. Chambers with $\text{Xe}+\text{CF}_4$ (1:1) gas mixture.

6.1 Nanosecond timing scintillation chamber with mixture $\text{Xe}+\text{CF}_4$ filling. The ratio $S1/S2$ for β and α -particles.

Recently we have investigated a scintillation signal ($S1$) and a ratio scintillation to ionization signal ($S1/S2$) for β and α -particles on prototype of fast chamber (see Fig.10) with mixture $\text{Xe}+\text{CF}_4$ (1:1) filling at a pressure of 10 bar. This chamber was irradiated with α (^{239}Pu) and β (^{63}Ni) particles. The scintillations signals ($S1$) were measured separately of photomultiplier (PMT-85) with fast shifter (OB-205). The ionizations signals ($S2$) were measured on anode of chamber. The addition in Xe of CF_4 and suppression of long triplet component of signals (27 ns) ensures the detection of scintillation singlet signals with high speed (1ns).

A shifter OB-205 has a maximum sensitivity range of 185 nm and converts with high efficiency of UV-light in visible light (420 nm). And also he have fast luminescence lifetime ($\sim 1\text{ns}$) and high photoluminescence quantum yield (99%). The measurements $S1$ signal used a fast amplifier and an oscilloscope Le Croy-232. Electronegative impurities O_2 , C_2F_4 and C_3F_8 were removed from the gases an a multistage purification system to a level of 10^{-8} O_2 equivalent (0,01 ppm). The entire system (chamber+ gas system) was checked by the "ISTOK" gas analyzer [32] for the presence of known electronegative impurities, which were not detected as a result.

For α -particles, the ratio $A=S1/S2$ was 0.63 and $B=S1/S2$ for β -particles 25.The ratio beta to alpha was $B/A=25/0,63=40$.

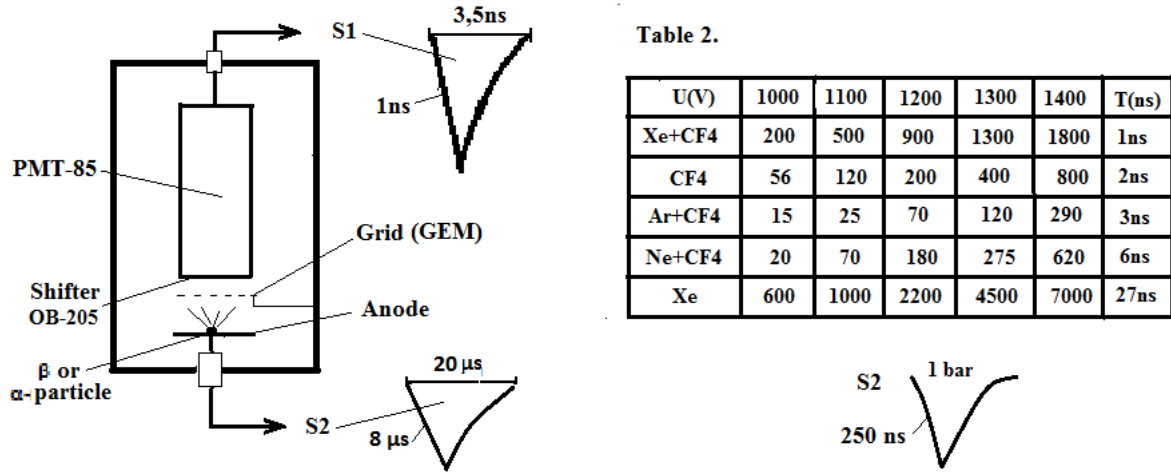


Fig.10. Left: prototype of fast chamber with mixture Xe+CF₄ (1:1) filling. Right: amplitude of scintillations signals (mV), which measured of photomultiplier for α -particles on different gases at pressure 10 bar. U (V) - voltage of PMT-85 (1000V – 1400V). The potential applied to anode is $V_a = +400V$, the gap of anode – grid is 8mm.

For mixture Ar+CF₄ (1:1) at a pressure 10 bar, the speed is 3 ns. For mixture Ne+CF₄ (1:1) at a pressure 10 bar, the speed is 6 ns (see Table 2). The ratio of scintillation signals α -particles to β -particles was $U(\alpha)/U(\beta)=2$. To get a electron multiplication factor (10^3) and large electroluminescence signals, the chamber instead of a grid is set to WGEM [9]. And to get a large electron multiplication factor (10^4 - 10^5) and large ionization anode signals, the chamber instead of a anode is set to system GEM+pin-anodes [16, 17, 21, 25].

6.2 The chamber with hole + pin-anode with Xe + CF₄ filling. The measurements photoelectron signals for α and β - particles.

The measurements were taken in the pin-anode chamber (Fig. 11 left) [20]. The chamber was used in two operating modes at cathode potentials $V_c = 0$ and -500 V. In both cases, cathode C2 was grounded. The results obtained thereby are presented in Fig.12. The wide peaks observed when α and β events were detected at $V_c = 0$ can be attributed to clouds of photoelectrons due to primary scintillations on particle tracks and to photoelectrons produced by photons from avalanches at the pin anode, as well as to ionization electrons from tracks of α and β particles (Fig.12 a). Since the concentration of photosensitive dopant CF₄ was high, all three peaks merged into a single wide peak, by contrast to the spectrum from the mixture of Ar + 40 ppm C₂H₄ in which these three peaks are recorded separately (see section 5.3).

Apparently, CF₄ photoionization takes place in the mixture of Xe+ CF₄: $h\nu (Xe_2^*) \rightarrow CF_4 \rightarrow e^+ + F + CF_3^-$. When a negative potential of -500 V is applied to chamber cathode C1, all photoelectrons gather on chamber cathode C2, and only ionization electrons from α and β particles are detected at the pin anode. Figure 11 (right) present the multiplication factor of ionization electron at the pin-anode in the chamber from α and β particles tracks as a function of the anode potential in the mixture Xe+CF₄ (1:1) at pressures of 1 and 10 bar. In these measurements, voltage $V_c = -500$ V was applied to cathode C1,

and cathode C2 was grounded. For 1 bar, the maximum electron multiplication factor equal to 3×10^4 was obtained for β particles and K_{\max} was obtained for α -particles.

The use of CF₄ dopant in noble gas with the aim of increasing the electron drift velocity was described in numerous papers [20]. Our results have demonstrated that CF₄ is a photosensitive dopant for Xe. As a result, it is possible to detect scintillations in a chamber filled with a mixture of Xe+CF₄ with a 100% geometrical efficiency, with is required in the experiment of the search for DM in the Universe for development of detectors with a high mass and complete suppression of background due to Kr⁸⁵ and external γ -rays. As well fluorine-19 (¹⁹F) has a large spin-dependent WIMP-proton cross-section [35, 36, 37].

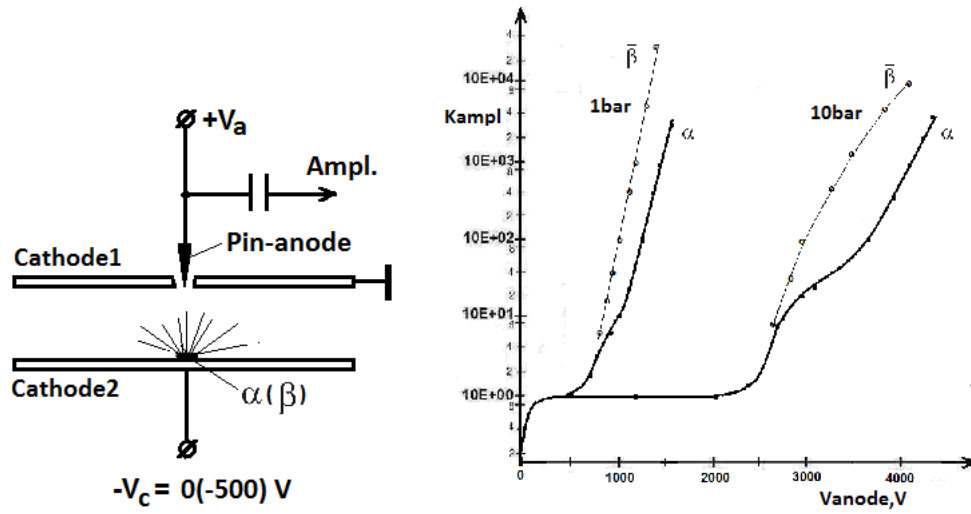


Fig. 11 Left: the chamber with Xe+CF₄ (1:1) filling [20]. Right: the multiplication factor of ionization electron at the pin-anode in the chamber from α (239Pu) and β (63Ni) particles tracks as a function of the anode potential (0 - 4500V).

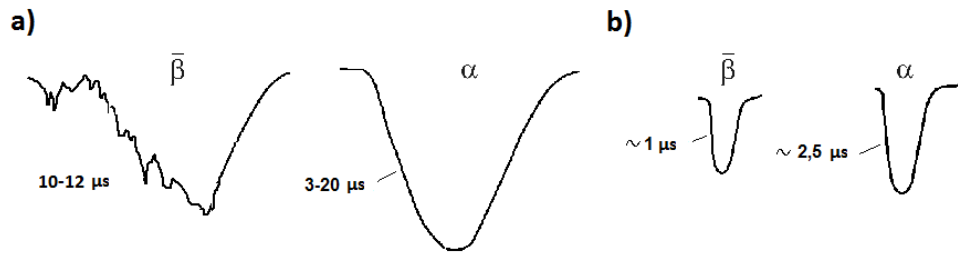


Fig.12. The signals of chamber with the mixture of Xe + CF₄ (1:1) filling at a pressure of 10 bar after irradiation with α and β particles at $V_a = 3000-4000$ V and (a) $V_c = 0$ V, (b) $V_c = -500$ V.

7. Search for spin-dependent WIMP-nucleon interactions.

7.1 Double-phase xenon chamber with a system GEM +pin-anodes.

In particle physics, the lightest supersymmetric particle (LSP) is the generic name given to the lightest of the additional hypothetical particles found in supersymmetric models. In models with R-parity conservation, the LSP is stable; in other words, it cannot decay into any Standard Model particle, since all SM particles have the opposite R-parity. There is extensive observational evidence for an additional component of the matter density in the universe, which goes under the name dark matter. The LSP of supersymmetric models is a dark matter candidate and is a weakly interacting massive particle (WIMP).

From the elementary particle physics in the framework of the standard Big Bang nucleosynthesis model one infers that DM consists mainly of WIMPs: massive neutrinos, axions and particles predicted by SUSY. The most probable candidates for the WIMP are the neutralino, predicted by supersymmetric theories (SUSY) [35].

The direct method for WIMP search consists in detection for their elastic scattering on detector nuclei. The WIMP interaction probability in detector can be represented in a form: $R = a_p W_p^2 + a_n W_n^2 + a_0 V^2$, where the first two terms determine the spin-dependent (sd) scattering and the last one is the spin-independent (si) scattering [35]. The ratio of the number of spin-dependent WIMP scattering R_{sd} to the number of spin-independent scattering R_{si} can be represented in a form:

$$R_{sd} / R_{si} = \eta_A \cdot \eta_{SUSY},$$

where η_A is determined by nuclear structure, and η_{SUSY} – by neutralino-quark interaction in SUSY model.

The dependence of η_A from atomic number A for nuclei (^1H , ^3He , ^{19}F , ^{73}Ge , ^{127}I , ^{205}Tl and others) with nonzero spins is shown in Fig. 13a (left) [35]. The dependence $R_{sd}(A)/R_{si}(\text{Ge}^{73})$ on neutralino mass are shown in Fig. 13a (right) for nuclei ^{19}F and NaI [36]. One can see that more strong restrictions on spin-dependent part of WIMP interactions can be obtained in experiment with ^{19}F (CF_4 , $\text{LAr}+\text{CF}_4$, $\text{LXe}+\text{CF}_4$) as compared with other nuclei [37]. The measurements are especially attractive in region of WIMP mass $8 \text{ GeV} \leq m_x \leq 14 \text{ GeV}$, where $R_{sd} > R_{si}$.

At present time a great experiments [24, 26-28] are carried out for WIMP search with detector containing nuclei LAr , LXe , NaI , Ge , the spin-independent (coherent) scattering for which is large [29]. One can see, that sensitivity of these experiments for spin-dependent scattering is 10-100 times less of expected effect as distinguished from coherent scattering experiments (see. Fig.13). The proposed in this work experiments increases the sensitivity of spin-dependent measurements to the point of the expected effect [23].

In this context, in our experiments [21, 25, 39] as another filling of the chambers for search of low-mass WIMP ($<10 \text{ GeV}/c^2$) and solar axions with spin-dependent interaction with deuterium (D_2), ^3He , ^{19}F and ^{21}Ne we propose to use the mixtures: $^{21}\text{Ne} + 10\%\text{H}_2$, $\text{D}_2 + 3\text{ppmTMAE}$, $^3\text{He} + 3\%\text{CH}_4$ at pressure 10-17 bar. And in our experiments [16-18] with liquid gases mixtures is used the mixtures with ^{19}F : $\text{LAr} + \text{CF}_4$ and $\text{LXe} + \text{CF}_4$ (see Fig. 14). The relative scintillation light outputs for investigated gases evaluated by an distribution area is shown in Table 3.

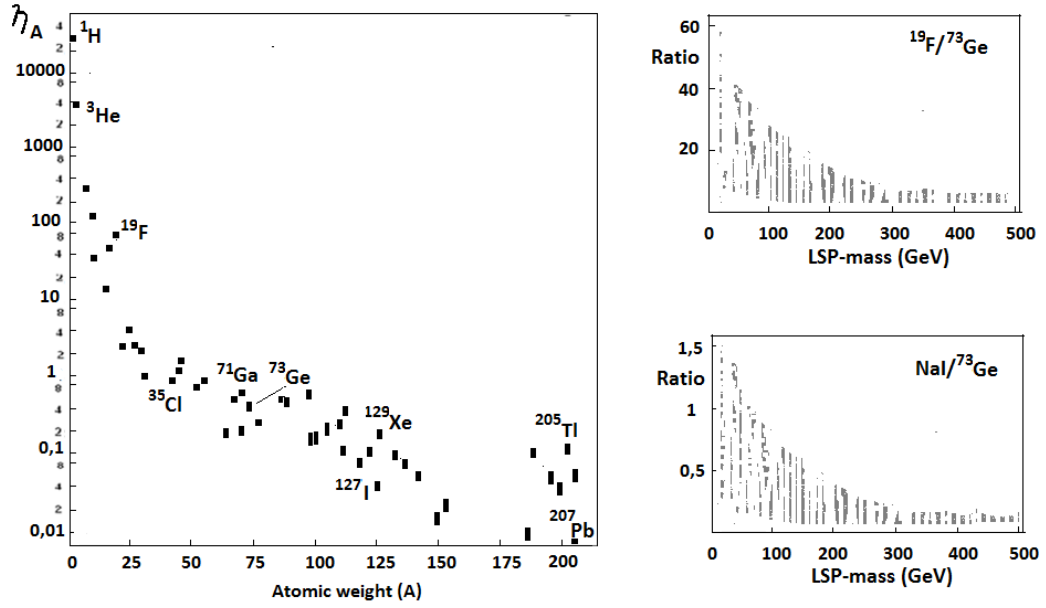


Fig. 13a. Left: The dependence of nuclear factor η_A from atomic number A for the nuclei with nonzero spins [35]. The high of symbols presents the change of η_A in a WIMP mass interval $10 \text{ GeV} \leq m_x \leq 500 \text{ GeV}$. Right: The dependence of $Rsd(A)/Rsd(^{73}\text{Ge})$ from WIMP mass for ^{19}F and NaI [36].

Gas	Xe gas	LXe	Xe+CF ₄	LXe+CF ₄	LCF ₄ /CF ₄	LAr+CF ₄ /Ar+CF ₄
Scintil. output	1	1	0,3	0,16	0,5	0,5

Table 3. The ratio of relative scintillation light outputs for different gases mixtures [44].

In this section, we describe a double-phase xenon chamber with a system GEM +pin-anodes and system of photomultipliers. Fig. 13b shows a design of the chamber.

To suppress the β , γ and n_0 background, we propose a comparison of scintillation singlet signal (S1) and ionization signal (S2) for every event is suggested. The addition in Xe of CF₄ and suppression of long triplet component of signals (27 ns) ensures the detection of scintillation signals with high efficiency and provides a complete suppression of the electron background. The singlet component S1 of the signal (1ns) is determined by the quenching factor (QF) of scintillation signals [47].

The scintillation intensity at the same particle energy is determined by the ratio 10: 5: 1 for electrons, protons and alpha particles [48]. That is, on the tracks of alpha particles, only 10% of their energy is spent on the singlet scintillation component. On the contrary, only 10% of the energy of beta particles is spent on ionization of the component, and 90% is the singlet scintillation component of the signals.

For alpha particles, the ratio $A=S1/S2$ was 0.63 and $B=S1/S2$ for beta particles 25. The ratio beta to alpha was $B/A=25/0,63=40$ for 50%Xe + 50%CF₄ gases mixture (see data of section 6.1 and 6.2).

It is possible that in mixture Xe + CF₄ the singlet component of signal (1ns) for beta particles with spin ($J_s=1/2$) is due to spin-dependent interaction between beta particles and molecules gases with non-zero spin (¹⁹F, ¹²⁹Xe, ¹³¹Xe). This assumption is indicated by a comparison of S1 and S2 for mixture 50%Xe + 50%CF₄ and mixture Ar + 40ppm C₂H₄ with zero-spin (see section 5.3). In the mixture Ar + C₂H₄, the average ratio of S1 to S2 does not exceed ten. The long triplet components of the signals are suppressed. In general, they do not depend on the spins of the particles, because they are determined by long secondary processes. For alpha particles with zero-spin the singlet component of signal (1,5ns) is not due to spin-dependent interaction.

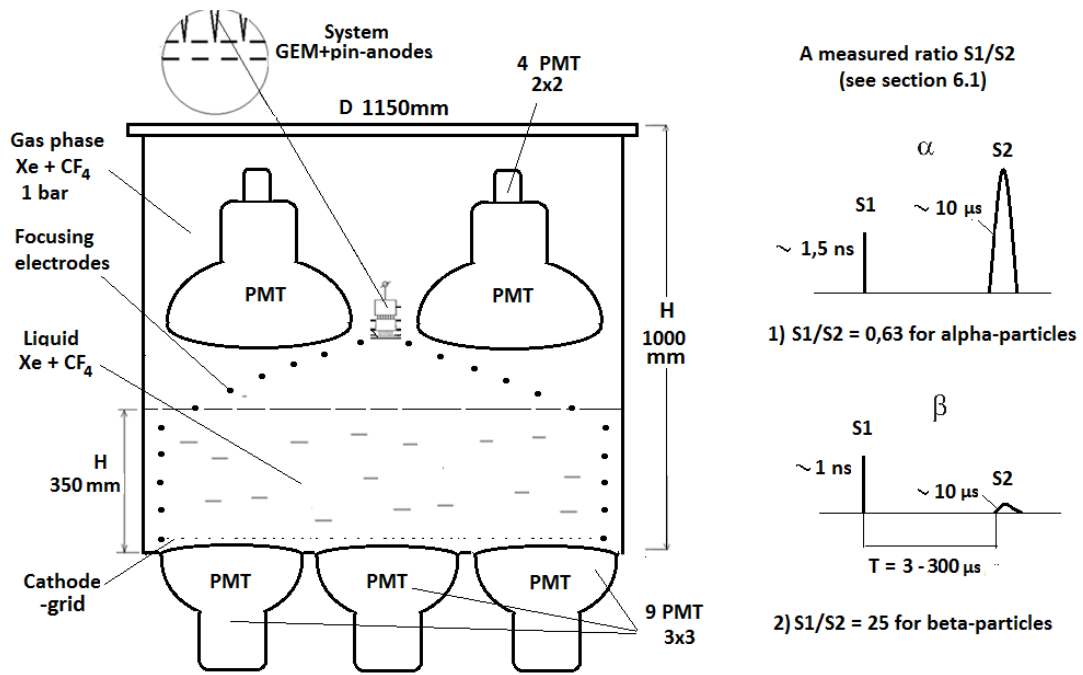


Fig. 13b. Double-phase Xe + CF₄ chamber with a system GEM + pin-anodes and photomultipliers.

The delay time between S1 and S2 is $T = 3-300 \mu s$, because: the drift time of electrons is $T = 0-300 \mu s$ in LXe + CF₄, and the drift time electrons is $T = 1-3 \mu s$ in gases phase 50%Xe + 50%CF₄ [44]. Electronegative impurities (O₂, C₂F₄, C₃F₈, etc.) removed from the gases an a multistage purification system to a level of 10^{-8} O₂ equivalent (0,01 ppm). The entire system (chamber+ gas system) is checked by the "ISTOK" gas analyzer [32] for the presence of known electronegative impurities.

7.2 The double-phase chamber with LCH₄ + TMAE mixture for search of spin-dependent WIMP-nucleon interactions.

In work [46] it is shown that the absolute lower bound for the rate of direct DM detection is due to the spin-dependent WIMP-nucleon interaction, and a new-generation experiment aimed at detecting DM with sensitivity higher than 10^{-5} event/(kg · day) should have a nonzero-spin target to avoid missing of the DM signal. In work is claimed that for targets with spin- nonzero nuclei it might be the spin-dependent interaction that determines the lower bound for the direct detection rate when the cross section of the scalar interaction, which is usually assumed to be the dominant part, drops below 10^{-12-13} pb particular, from this work one can see that all fluorine-containing targets (LiF, CF₄, C₂F₆, and CaF₂, etc.) have almost the same sensitivity to both the SD and SI WIMP-nucleus interactions.

Among all materials considered a detector with a ^{73}Ge , ^{129}Xe , or NaI target has better prospects to confirm or to reject the DAMA result [29] due to the largest values of the lower bounds for the total rate $R(10, 50) > 0.06 - 0.08$ events/(kg day). If, for example, one ignores the SI WIMP interaction, then all materials have almost the same prospects to detect DM particles with the only exception of CH_4 (see Fig. 14). The results obtained are based on previous evaluations of the neutralino-proton (neutron) spin and scalar cross sections for the neutralino masses $m_\chi < 200 \text{ GeV}/c^2$.

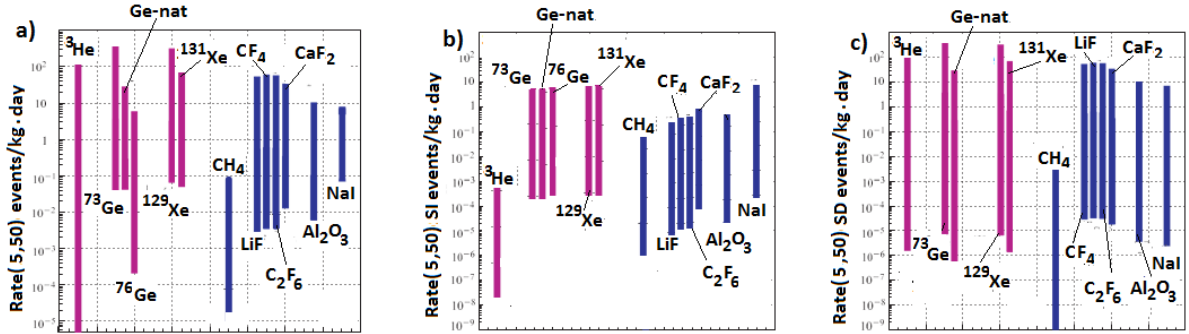


Fig. 14: a) variations of expected event rates, $R(5, 50)$, for a number of targets followed from the DAMA-allowed cross sections σ_{SD} and σ_{SI} . Targets with nonzero-spin nuclei from the odd-neutron (odd-proton) group model are given in the left (right) part of the figure; b) variations of expected spin-independent contributions to the event rate, $R(5, 50)_{\text{SI}}$, in a number of targets followed from the DAMA-allowed cross sections σ_{SD} and σ_{SI} ; c) the same as in b, but for the spin-dependent contributions $R(5, 50)_{\text{SD}}$ [46].

In this context, in our experiment [15] with liquid CH_4 as another filling of the chamber for search of low-mas WIMP ($< 10 \text{ GeV}/c^2$) we propose to use the mixture $\text{LCH}_4 + 40\text{ppmTMAE}$ (see Fig. 15).

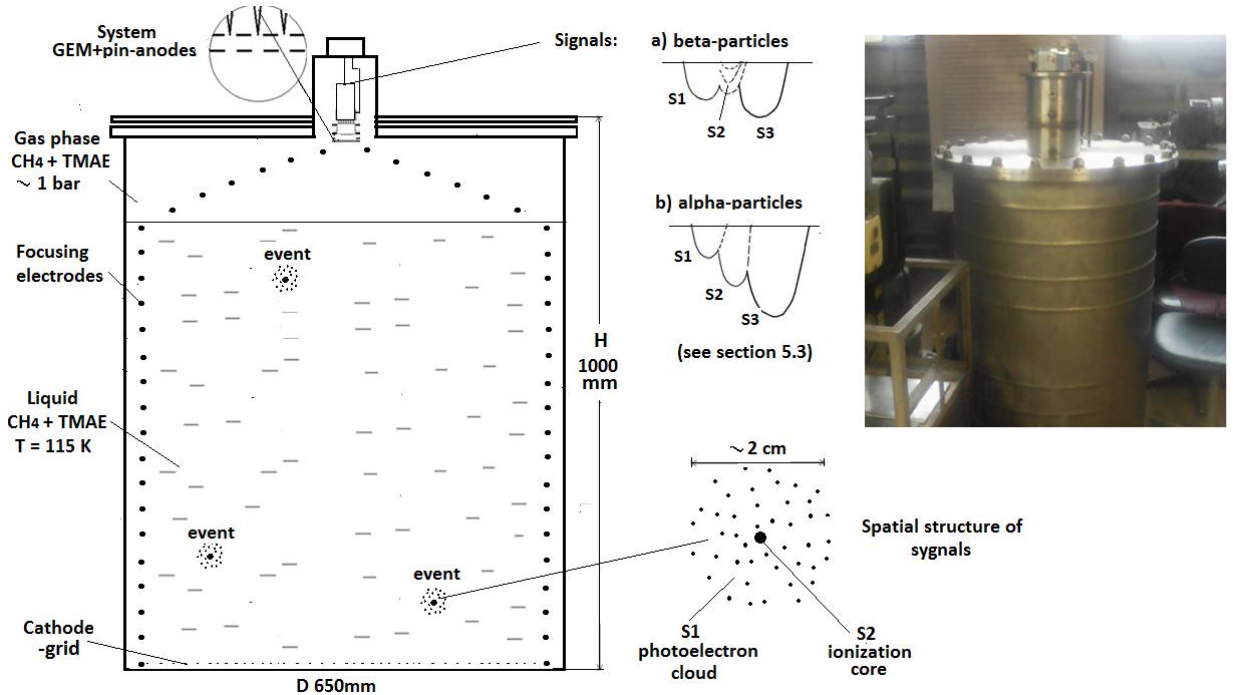


Fig. 15. A liquid-methane ionization chamber with a system GEM + pin-anodes for search of spin-dependent WIMP-nucleon interactions.

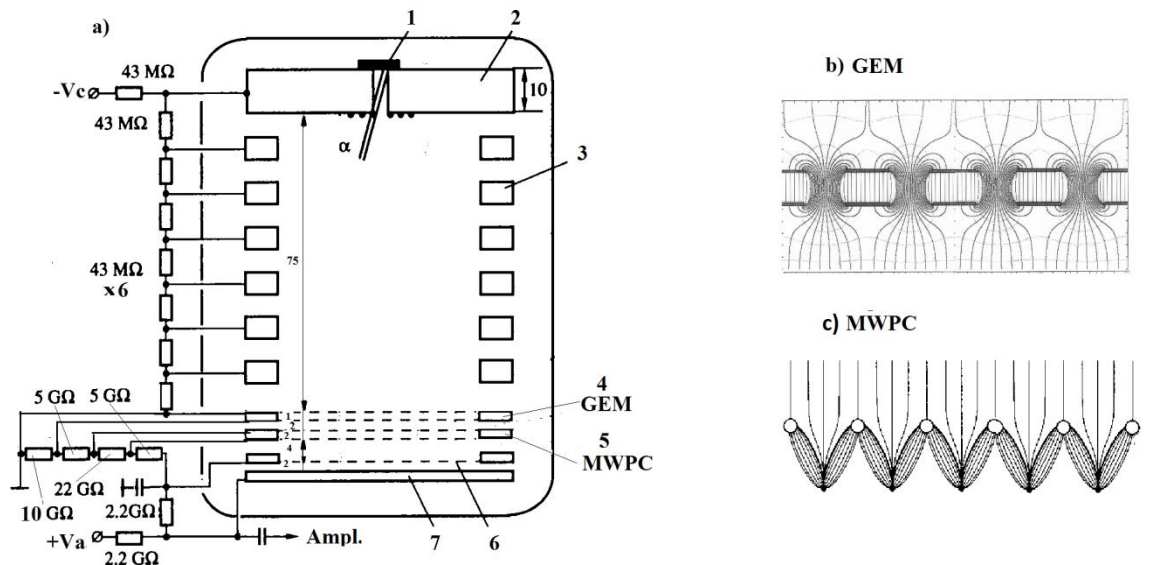
The body of the chamber is made of titanium. The cathode-grid of the chamber is immersed in liquid methane. The layer of liquid methane above the cathode is equal to 800 mm. The temperature of liquid methane is equal to 115 K and the pressure of gaseous methane over the liquid methane is equal to 1,3 bar for this temperature. The system GEM + pin-anodes is placed in gaseous methane. The addition in liquid CH₄ of photosensitive TMAE [19] and suppression of triplet component of scintillation signals ensures the detection of scintillation signals with high efficiency and provides a complete suppression of the electron background (see section 5.3).

8. Time-projection chamber with high dE/dz and energy resolutions.

It is known that multi-wire proportional chambers (MWPC) used in time-projection chambers (TPC) fail to provide good energy resolution [34]. This is mainly due to the fact that multiplication of ionization electrons occurs in chamber regions with different electric field intensities resulting in variation of the multiplication factor. Additionally, the MWPC features a low dE/dz resolution in the drift direction of the ionization electrons due to slow motion of positive ion clouds from anode wires.

In our paper [38], we describe a TPC with both high energy and dE/dz resolutions. Fig. 16a shows a design of the chamber. The chamber contains the cathode 1 with a 4-mm-diameter collimating opening, behind which a ²³⁹Pu source with a 10⁵ flow rate is installed at a distance of 10 mm. The rings 3 provide a uniform drift field. The MWPC 5 used for electron multiplication contains the cathode MWPC wound with a 2-mm pitch of a beryllium bronze 100- μ m-diameter wire. The anode is wound of a 20 μ m diameter W + Au wire with a 2 mm pitch. The MWPC gap is 2 mm. In projection, the anode wires are exactly in the middle between the cathode wires. The chamber contains cathode 6 and anode 7 of the measurement gap. The maximum electron multiplication factor for α -particles is $\sim 10^3$. To get the total electron multiplication factor (10⁵), the chamber is set to MGEM 4 with the etching of holes [14].

Due to the photon mechanism, when the avalanche evolves in the anode MWPC wire, an electron charge proportional to the initial ionization charge appears in the transfer gap between the electrodes 5 and 6. This charge drifts towards the measurement gap between the electrodes 6 and 7. Electrodes 6 and 7 are wound of a 100 μ m diameter wire with a 1 mm pitch. The width of the gap 5-6 is 4 mm. The electric field intensity in this gap is insufficient for evolving avalanches and the gap records the electrons without multiplication, i.e., in the induction operation mode of the ionization chamber.



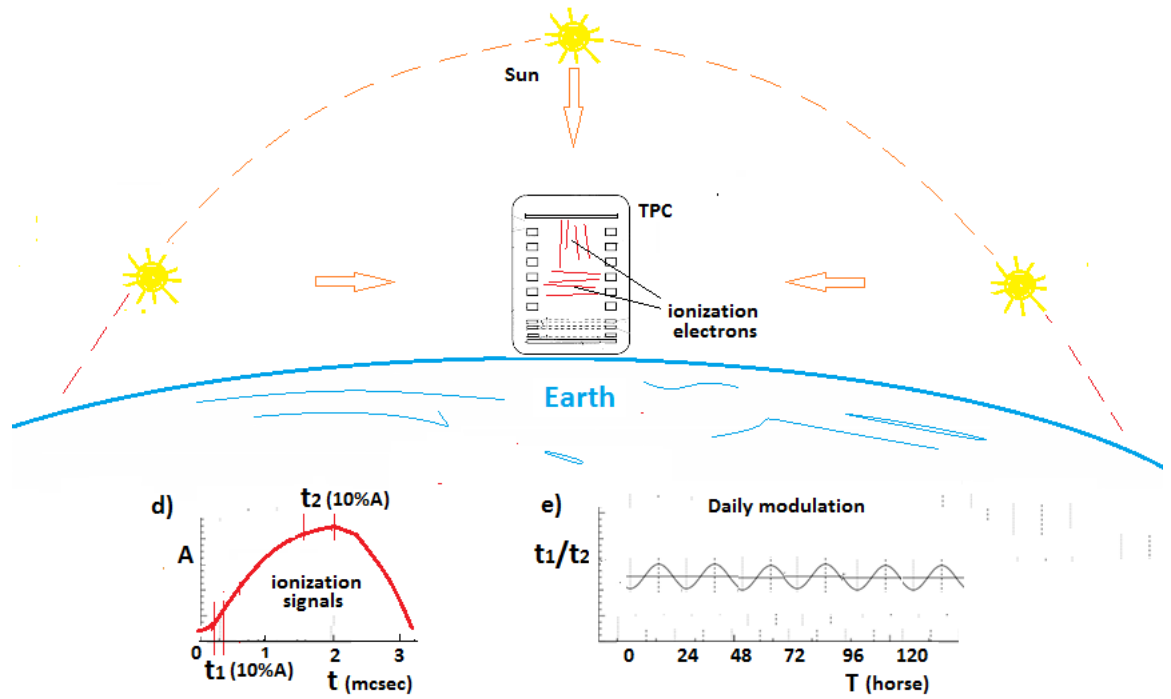


Fig.16. Design of time projection chamber (TPC) with MWPC and GEM (a), electric field structure in the GEM (b), MWPC (c), signals of TPC (d) and daily modulation of signals (e).

Fig. 16 (b, c) shows the electric field structure in the MWPC and GEM gaps. Since the electric field intensity in the MWPC gap is much higher than in the drift gap and due to the symmetric location of the cathode relative to the anode wires, the electric field lines, when passing from the drift gap to the MWPC gap, concentrate into a narrow beam, which is orthogonal on the average to the anode plane and sufficiently uniform. As a result, the electron multiplication occurs in a more homogeneous electric field than in usual MWPCs, in which the electric field lines meet the anode wires at different angles in different MWPC regions and have different average densities.

In the process of its evolution, the avalanche discharge involves about 180° of the anode wire in the azimuth. In our case, conditions for the evolving discharge are the same for all ionization electrons within the drift gap, because the field distributions on all wires are identical, and the fields are more homogeneous (see Fig. 16 d, e).

Since, for usually utilized mixtures, the electron drift speed in the measurement and drift gaps is $\sim n \cdot 10^6$ and $\sim n \cdot 10^5$ cm/s, respectively, and the measurement gap is small, the calculated dE/dz resolution referred to the TPC drift gap appears to be sufficiently high: the chamber resolves the track regions or separate tracks spaced by ~ 0.2 mm.

In order to determine the energy resolution and signal structure the chamber was filled with an Ar + 0.5% C₂H₂ + 10%CH₄ mixture at a total pressure of 3,5 bar. When recording α -particles from a ²³⁹Pu source, the energy resolution was 8.1% (half-intensity half-width). The front of signals was 2 μ sec. (Fig.16d).

Three anode grids with 0,2mm pitch and 0,2mm gaps may be placed in the ionization chamber for detection of x, y and 45° x-coordinates. The electrons are moving after multiplication through three anode grids inducing on them the signals. The errors for x, y-coordinates will be equal to 0,2mm and error for z-coordinate will be 0,2mm (not including diffusion errors).

The method allows you to measure the direction of movement of particles. In our work [45] we have study of TPC with the Penning mixture He+3%CH₄ filling at a pressure 17 bar for direct detection of solar neutrinos. As another filling is use the mixture ³He + 3%CH₄ for search of SD-interactions. As well time projection chamber with the mixture D₂ + 3ppmTMAE filling at a pressure 10-20 bar allow to search of spin-dependent interactions of solar axions and deuterium [21, 23, 25].

Finally, we compare this chamber with existing multistage avalanche chambers, which also provide high energy and dE/dz resolutions and with the MICROMEGAS chambers [7]. The MWPC used in our chamber in place of the avalanche chamber allows it to operate under an increased pressure of the filling gas (up to 10-20 bar), whereas other chambers are intended for operation mostly at pressures lower than the atmospheric pressure. The high resolution (dE/dx, dE/y, dE/z) of the TPC allows you to measure the direction of the flow of solar neutrinos and axions. Directionality allows to use only electrons recoiling away from the sun, effectively eliminating most background events.

9. Detecting chamber with system GEM+pin-anodes for search of narrow pp-resonances (quarks) at the accelerators in the energy region 150 – 300 MeV.

The existence of narrow peculiarities in a two-proton system was observed for the first time by JINR scientists in nucleon reactions with π -mesons production [40]. By now the statistics has substantially been enlarged by this group and narrow pp-peaks at the level 3-5 standard errors have proved to be present in various reactions within a wide energy range [41]. Analyzing the effective mass distributions in the system of particles $n\bar{p}$, $\pi^+\pi^-$, $\pi^+\pi^+$ from inelastic reactions with π -mesons production this group also found the narrow peculiarities, excitation energies of which were just the same as those for pp-system. By now this group has observed narrow π^- p-resonances which excitation energies coincide well with those of pp-systems. In work [42] Y.A.Troyan group has observed the existence of narrow pp-resonances in elastic pp-scattering differential cross-section within 116-199 MeV.

The results are compared with the data of various experiments of elastic scattering at the energy region 0,2 - 10 GeV/c² (Fig. 17).

The experiment with MPWC which detectors the recoil protons with mixture Xe + iC₄H₁₀ (1:1) under a pressure 15 torr we proposed in year 1993 to search for narrow pp-resonances (quarks) in the energy region 150 – 300 MeV at the MMF accelerator [43]. In the experiment the external proton beam of the accelerator is used with the energy changed from 160 MeV to 300 MeV, intensity 2×10^{11} protons per second and energy spread 0,5 MeV (FWHM). The formed proton beam goes through the tube filled with hydrogen (H₂) under a pressure of 5 bar (see Fig.13). Recoil protons from the elastic pp-scattering are detected at angles 70° laboratory system for coincidence with gas proportional and scintillation detectors. Detectors adsorb the recoil protons with the energies up to 35 MeV. This experiment requires high speed of ionization electrons collection time and respectively, the detector resolution time is about 10⁻⁸ sec.

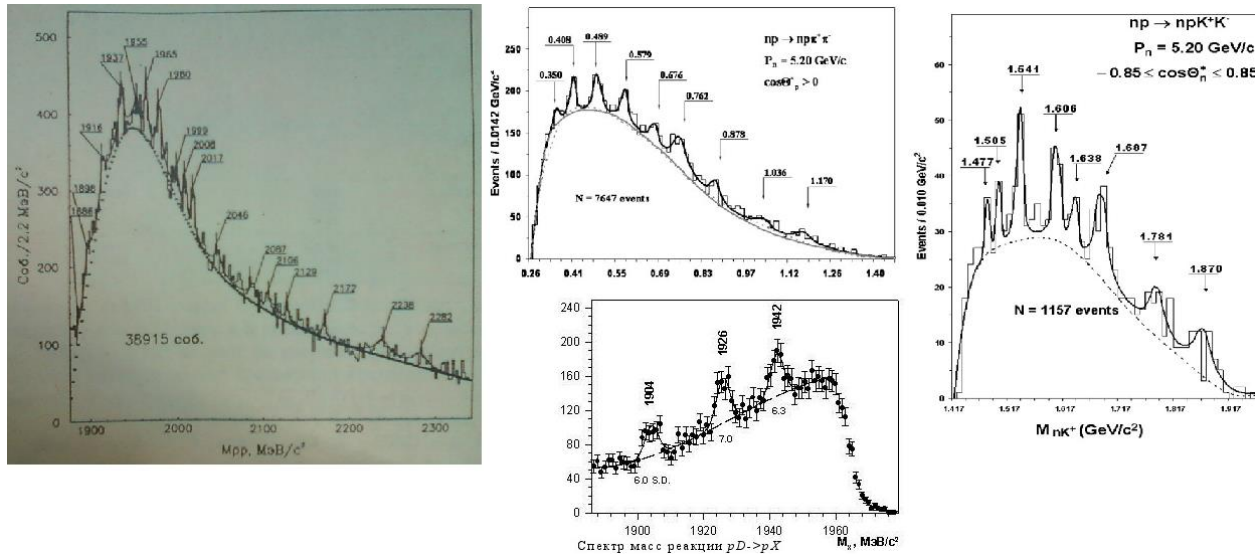


Fig. 17. The results of experiments JINR (Dubna) and MMF (INR, Moscow).

We propose detect the recoil protons with the energies up to 35 MeV on scintillation chamber (see section 6.1) with Xe+CF₄ (1:1) filling under a pressure 50 torr and ionization chamber with system GEM+pin-anodes under a pressure 15 torr (see Fig.18). Signals are picked up from the scintillation and ionization chamber by fast amplifier and then are transferred to coincidence and anticoincidence circuits with a resolving time 10^{-8} sec. When the signal from the scintillation chamber coincides with that from the ionization chamber the signal amplitude of the latter is registered by the amplitude analyzer. Its readings determine the total number of the events at a certain energy and detection angle ($N_{\text{events}} + N_{\text{backgr}}$). The ratio $N_{\text{events}}/N_{\text{backgr}}$ is determined an elastic peak against the background.

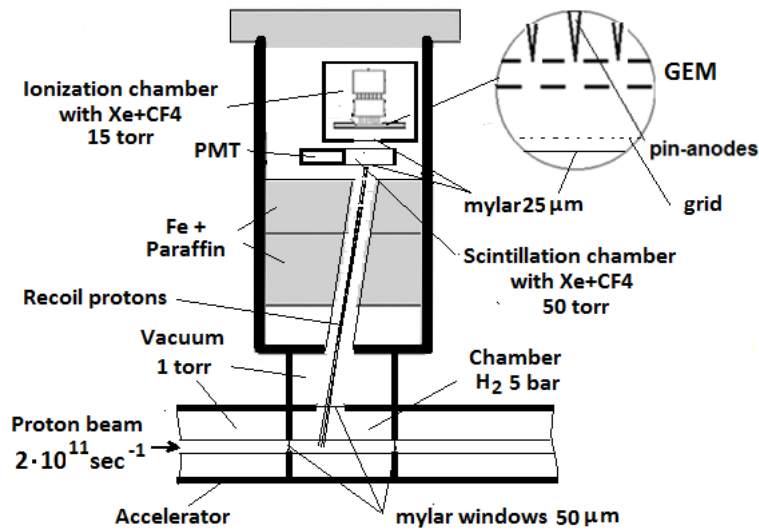


Fig.18. Experimental setup with scintillation and ionization chambers.

We would like to mention that chambers with system MGEM+pin-anodes, as far as the MWPC [1] can have many applications for detecting events in high energy physics experiments.

10. Operation principle of MWPC, GEM and system GEM+pin-anode

The operation principle of Multi-Wire Proportional Chambers (a), GEM (b) and system GEM + pin-anode (c) is illustrated in Fig.19. The factors which have allowed us to obtain high electron multiplication factors in the GEM + pin-anode system are as follows:

- (1) High electric field strength in the system GEM + pin-anode makes it possible to obtain a big length of electron avalanche and high value of the electron multiplication factor (10^6 - 10^7);
- (2) Positive ions from the avalanche at the pin are transferred by the electric field, mainly, to the walls of the hole in which the pin is located and, in smaller quantities, towards the ionization electrons being collected at the pin, which rules out the possibility of streamers being developed at the interface
- (3) For GEM (see technology b) extraction efficiency decrease at low transfer fields values due to a worst electron extraction capability from the lower side of the GEM [32];
- (4) Absence of a plastic insulation excludes the emergence of leakage current and spark breakdown between electrodes. Accidental spark events in such system don't lead to their failure as positive ions quickly move away from breakdown by a strong electric gap field.

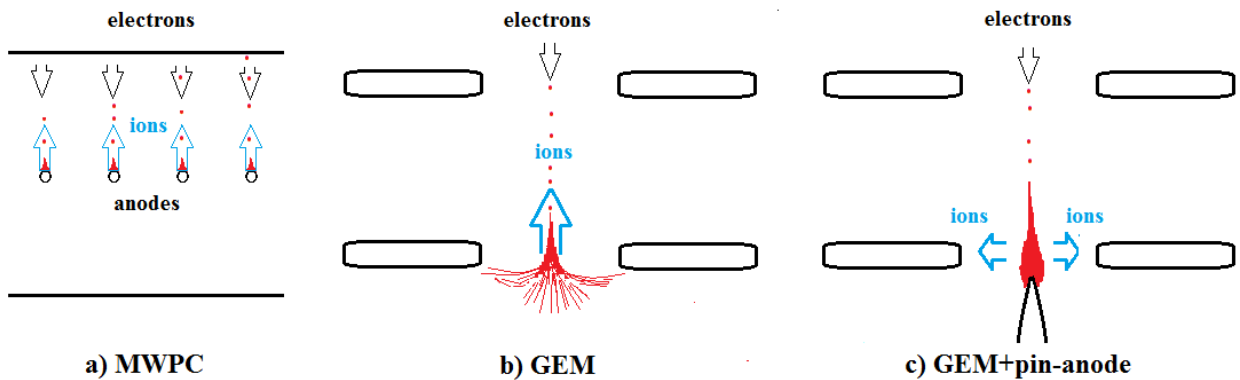


Fig.19. Operation principle of Multi-Wire Proportional Chambers (a), GEM (b) and GEM+pin-anode (c). Electron avalanches are shown for three technologies (a, b, c); red paths are electron trajectories, also the drift of ions is indicated (blue paths).

The leading edges of the signals picked off the pin-anode are 1-3 μ s on different gases and their mixtures; however, signal differentiation helps extract the initial parts of the edges 0,2-0,3 μ s long. The steepness of the pulse leading edges at the pin-anode is determined by the geometry of the pin-hole geometry and the potential difference between them. The high electric field strength near the pin-anode ensures a fast removal of an envelope of positive ions from pin, which, in combination with the small gaps between the pin and the walls of the hole-cathode ($\sim 0,4$ mm), ensures a rapid decrease in amplitude of the signal induced at the pin-anode by the positive ion envelope; i.e., it guarantees a high steepness of the pulse leading edge ($\sim 1\mu$ s).

We have also plans for constructing of large scale (150mmx150mm) MGEM + pin-anodes detectors (see Fig.20).

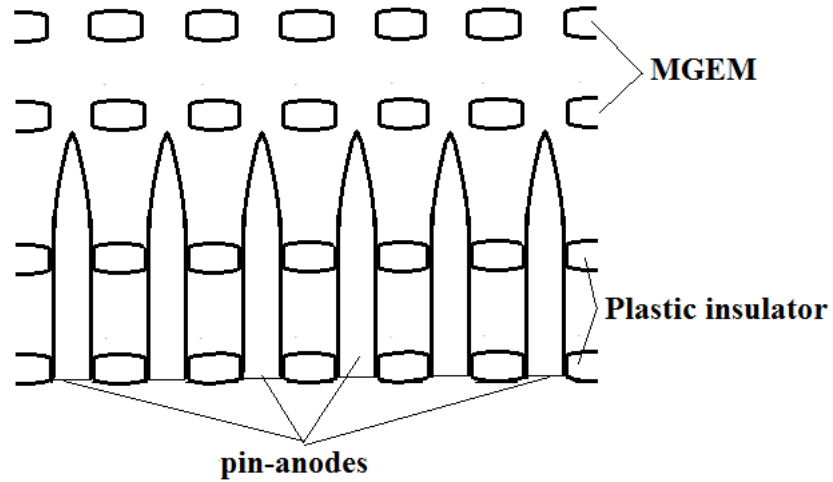


Fig.20. Schematic drawing of system GEM + pin-anodes in which plastic insulator contains of holes for pin-anodes. The metal electrodes (MGEM) made by a method of drawing a mask on brass plates.

11. Discussion

In works of CERN the multichannel gas electron multipliers consisting of a plastic plate 50-2000 microns thick with metal or high-resistive thin (some microns) deposits from two parties are presented [2-4]. These GEMs provide the best spatial resolution and higher rate than wire chambers. However, an essential disadvantage of these GEMs consists in their low reliability and stability. The matter is that at cathode dispersion by positive ions from proportional avalanches in GEM with metal or high-resistive electrodes there is a sedimentation of the sprayed carrying-out material on walls of holes, which leads to subsequent leaks and breakdowns between electrodes.

In our works we have studied the Penning mixtures: He + 3% CH₄, Ne + 30% H₂, Ar + 10% Xe, Ar + 10% H₂, 50% He + 50% Ne [45] and Ar(Xe) + 20% CF₄, LAr(LXe) + 20% CF₄ [44].

In this work we propose as another filling of the chambers for search of low-mass WIMP (<10 GeV/c²) and solar axions on spin-dependent interaction with deuterium (D₂), ³He, ¹⁹F and ²¹Ne is used the mixtures: ²¹Ne + 10% H₂ [21], D₂ + 3ppmTMAE [25], ³He + 3% CH₄ [39] at pressure 10-17 bar. And in our experiment with liquid mixtures [16-18, 37, 44] is used the mixtures LAr + CF₄ (¹⁹F) and LXe + CF₄ (¹⁹F, ¹²⁹Xe, ¹³¹Xe).

The time projection chamber [38] with the mixture D₂ + 3ppmTMAE filling at a pressure 10 bar allow to search of spin-dependent interactions of solar axions and deuterium (section 8).

In work [46] is claimed that for targets with spin- nonzero nuclei it might be the spin-dependent interaction that determines the lower bound for the direct detection rate when the cross section of the scalar interaction, which is usually assumed to be the dominant part, drops below 10⁻¹²- 10⁻¹³ pb. In particular, from this work one can see that all fluorine-containing targets (LiF, CF₄, C₂F₆, and CaF₂, etc.) have almost the same sensitivity to both the SD and SI WIMP-nucleus interactions. Among all materials considered a detector with a ⁷³Ge, ¹²⁹Xe, or NaI target has better prospects to confirm or to reject the

DAMA result [29] due to the largest values of the lower bounds for the total rate $R(5, 50) > 0.06 - 0.08$ events/(kg day). If, for example, one ignores the SI WIMP interaction, then all materials have almost the same prospects to detect DM particles with the only exception of CH_4 . In this context, in our experiments [15] with liquid CH_4 as another filling of the chamber for search of low-mas WIMP ($< 10 \text{ GeV}/c^2$) we propose to use the mixtures $\text{LCH}_4 + 40\text{ppmTMAE}$ (section 7.2).

12. Summary & Outlook

In our works [9-14] GEMs with wire (WGEM) or metal electrodes (MGEM) and gas gap between metal electrodes without plastic were realized. An absence of a plastic insulation between electrodes of these GEMs excludes leakage currents and spark breakdowns between the electrodes.

In our works [16, 17, 21, 25] it was suggested to search low mass WIMPs and solar axions with help of chambers with GEMs and systems WGEM (MGEM) + pin-anodes. In work [18] we proposed a addition in liquid Xe (Ar) of photosensitive dopants and a comparison of scintillation (S1) and ionization signals (S2) for every event is suggested. In our works [15, 25, 37] it was suggested that the search for spin-dependent WIMP-nucleon interactions with help of detecting system GEM + pin-anodes can be performed.

In that respect we would like to add the next important comments:

1. As far as WIMPs with large masses ($> 10 \text{ GeV}$) experimentally were not found so far [24, 27, 29, 31], it is necessary to search the WIMP with small masses ($\leq 10 \text{ GeV}/c^2$).

2. The data of the new DAMA/LIBRA–phase2 confirm a peculiar annual modulation of the single-hit scintillation events in the (2–6) keV energy range (WIMP mass $< 10 \text{ GeV}/c^2$) satisfying all of the multiple requirements of the Dark Matter [29]. J.Va’vra have supposed [31] that this effect is explained by low mass WIMP ($\sim 1 \text{ GeV}/c^2$) scattering on protons in H_2O molecules (H^+).

3. In this context, in our experiments [15] with liquid CH_4 as filling of the chamber for search of low-mas WIMP we propose to use the mixture with ^1H ($\text{LCH}_4 + 40\text{ppmTMAE}$). As well as, it is necessary to search of WIMP with small masses ($\leq 10 \text{ GeV}/c^2$) in spin-dependent interactions between DM particles and gases with nonzero-spin nuclei (D_2 , ^3He , ^{19}F , ^{21}Ne , ^{129}Xe , ^{131}Xe) [46].

Finally, we would like to mention that MGEMs can have various applications in medicine. Such MGEMs can be used in different medical instruments for their use in X-ray surgery or Positron Emission Tomography (PET), where a high operation stability and reliability of the whole complex of instrument is required. Recently we have proposed a PET system, based on these MGEMs and BaF_2 -crystals [49].

References.

[1] G. Charpak and F. Sauli, Physics Letters 78B (1978) 523.

[2] R. Bouclier et al, “The Gas Electron Multiplier (GEM)”, IEEE Trans. Nucl. Sci. NS-44, 646, 1997.

- [3] F. Sauli, "GEM: A new concept for electron amplification in gas detectors", Nucl. Inst. Meth., A386, 531, 1997.
- [4] F. Sauli, "The gas electron multiplier (GEM): Operating principles and Applications", Nucl. Instrum. Meth. A805, 2016.
- [5]. L. Periale et al, Nucl. Instrum. Methods A 478, 377 (2002).
- [6]. R. Chechik et al, Nucl. Instrum. Methods A 535, 303 (2004).
- [7]. A. Breskin et al, Nucl. Instrum. Methods A 598, 107 (2009).
- [8]. A. Di Mauro et al, Nucl. Instrum. Methods A 581, 225 (2007).
- [9] B.M.Ovchinnikov, V.V.Parusov, "A Multichannel Wire Gas Electron Multiplier", Instruments and Experimental Techniques, Vol.53, №5 (2010), 653-656.
- [10] B.M.Ovchinnikov, V.V. Parusov, "Multichannel gas electron amplifier" Patent of Russia RU 2417384, 11.03.2010.
- [11] B.M.Ovchinnikov, V.V.Parusov, " Multichannel Wire Gas Electron Multipliers with 1 and 3mm Gaps", Instruments and Experimental Techniques, Vol.53, №6 (2010), 836-839.
- [12] "B.M.Ovchinnikov, V.V.Parusov, "Multichannel Wire Gas Electron Multipliers", Instruments and Experimental Techniques, Vol.56, №6 (2013), 634-636.
- [13] B.M.Ovchinnikov, V.V.Parusov, "Multichannel gas electron amplifiers with metal electrodes", Instruments and Experimental Techniques, Vol.54, № 1(2011),43-46.
- [14] D.S.Kosolapov, B.M.Ovchinnikov, V.V.Parusov, V.I.Razin, "Multichannel gas electron amplifiers with metal electrodes", Instruments and Experimental Techniques, Vol.56, № 6(2013), 684-685.
- [15] V.A.Bednyakov, B.M.Ovchinnikov, V.V.Parusov, "Methane ionization chamber to search for spin-dependent dark matter interactions", arXiv:hep-ph/0508052v1, 4 Aug 2005.
- [16] B.M.Ovchinnikov, V.V. Parusov, "Methods for detecting events in double-phase argon chambers", Instruments and Experimental Techniques, Vol.56, № (2013), 516-520.
- [17] B.M.Ovchinnikov, Yu. B. Ovchinnikov, V.V. Parusov, "Massive Liquid Ar and Xe Detectors for Direct Dark Matter Searches", JETP Letters, 2012, Vol.96, №. 3, pp. 149-152.
- [18] B.M.Ovchinnikov, V.V.Parusov, "A method for background reduction in an experiment for WIMP search with a Xe(Ar) – liquid ionization chamber", Astroparticle Physics 10 (1999) 129.
- [19] D.F.Anderson, "New photosensitive dopants for liquid argon", Nucl. Instrum. Methods Phys. Res. A245, 361 (1986).
- [20] B.M.Ovchinnikov, V.V.Parusov, "A Study of Ar + C₂H₄ and Xe + CF₄ Gas Mixtures", Instruments and Experimental Techniques, Vol.56, № 6(2013), 637-639.

- [21] B.M.Ovchinnikov, I.I.Tkachev, V.V. Parusov, "The Methods for Direct Detection of WIMP with Mass <0.5 GeV", Physics Journal, Vol. 1, No. 2, July 2015, pp. 31-34.
- [22] I. Giomataris, I. Irastorza, I. Savvidis et al., "A novel large-volume Spherical Detector with Proportional Amplification read-out" // JINST 3:P09007, 2008
- [23] V.A.Bednyakov, B.M.Ovchinnikov, V.V.Parusov, "Search for spin-dependent interaction of Dark Matter particles", Preprint INR №1144/2005.
<https://cds.cern.ch/record/865973/files/0508052.pdf>
- [24] L.Baudis, "WIMP dark matter direct-detection searches in noble gases", Physics of the Dark Universe (2014) 4 50-59
- [25] B.M.Ovchinnikov, V.V. Parusov, "Search for Low Mass WIMP and Axions, Emitted from the Sun" Universal Journal of Physics and Application, Vol. 10(2), 2016, pp. 58 – 59.
- [26] K. Abe, K. Hieda, K. Hiraide et al., "Search for solar axions in XMASS, a large liquid-xenon detector", Physics Letters B 721 (2013) 46-50.
- [27] E. Aprile et al., "The scintillation and ionization yield of liquid xenon for nuclear recoils" arXiv: 0807.0459v2 [astro-ph], 31 Dec 2008. (10.1016/j.nima.2008.12.197).
- [28] R. Bernabei, P. Belli, F. Cappella, V. Caracciolo, S. Castellano, R. Cerulli, C. J. Dai and A. d'Angelo, "Final model independent result of DAMA/LIBRA-phase1", Eur. Phys. J. C73 (2013) 12, 2648R.
- [29] R. Bernabei et al. "Improved model-dependent corollary analyses after the first six annual cycles of DAMA/LIBRA-phase2", Nuclear Physics and Atomic Energy, 20(4), 317-348 - December 2019.
- [30] R.K.Janev, W.D.Langer, K.Evans et al., "Elementary Processes in Hydrogen-Helium Plasmas", Springer Verlag, Berlin, Heidelberg, New York, London, Paris, Tokyo.
- [31] J. Va'vra, "A New Possible Way to Explain the DAMA Results", Physics Letters B 735 (2014)181.
- [32] F.Murtas, "Development of a gaseous detector based on Gas Electron Multiplier (GEM) Technology", LNF-INFN, 28 Nov 2002.
- [33] Ovchinnikov B.M., Parusov V.V. "A device to measure the total content of electrically negative impurities in gases, that are not electrically negative". Instruments and Experimental Technique. 1995. T. 38. № 1. C. 183-189. Patent of Russia RUS 2258924 29.06.2004
- [34] A.Bondar et al. "Light multi-GEM detector for high-resolution tracking systems" Nucl.Instrum.Meth.A556:495-497, 2006.
- [35] V.A. Bednyakov, H.V. Klapdor-Kleingrothaus, S.G. Kovalenko, Phys. Lett. B329 (1994) 5.

- [36] V.A. Bednyakov, H.V. Klapdor-Kleingrothaus, S.G. Kovalenko, Phys. Rev. 50, N 12 (1994) 7128.
- [37] B.M. Ovchinnikov, V.V. Parusov, "Freon-filled detectors", Instruments and Experimental Techniques 39 (1996):795-798.
- [38] B.M.Ovchinnikov, V.V.Parusov, "Time-projection chamber with high dE/dz and energy resolutions", Instruments and Experimental Techniques, Vol.43, № 1, 2000, pp. 24-25.
- [39] B.M. Ovchinnikov, V.V. Parusov "Search of the WIMP and Ge^{76} 2β -decay with high pressure chamber. Prototype of solar neutrino detector" Preprint INR RAS 0944/1997.
- [40] K.Beshliu et al., Preprint JINR . DI83-815, Dubna, 1983, K. Beshliu et al., "Channel cross section of np interaction reactions with $P_n = 1-5 \text{ GeV}/c$," Sov. J. Nucl.Phys. 43, 565–568 (1986)
- [41] Yu.A.Troyan et al. Proc. 10 Int. Seminar on High Energy, Dubna, 1990, p.149.
- [42] Yu.A.Troyan et al., Yadernaya fizika, vol.54, issue 5 (1991) 1301.
- [43] V.N. Aseev , S.V. Dvortsov , V.A. Krasnov, B.M. Ovchinnikov, P.N. Ostroumov, V.V. Parusov "Proposal of the experiment on search for narrow pp-resonances in differential cross-section of elastic pp-scattering at small angles within the energy region below meson-production threshold" Preprint INR RAS 814/1993.
- [44] B.M.Ovchinnikov, V.V.Parusov, "The preparing of an experiment for search the spin-dependent interaction of WIMP", Preprint INR №1097/2003. Russian version: Preprint INR №1067/2001.
- [45] B.M. Ovchinnikov, V.V. Parusov, "Investigation of the proportional discharge mechanism in nonelectronegative gases" Nucl. Instrum. Methods A 485, 539 (2002).
- [46] V.A. Bednyakov, "Spin in Dark Matter Problem", Physic of elementary particles and atomic nucleus, 2007, T.38. 3.
- [47] J. B. Birks, The Theory and Practice of Scintillation Counting, Pergamon Press, London, 1964.
- [48] Chemist`s handbook, p.154, www.chem21.info.
- [49] B.M. Ovchinnikov, V.V. Parusov, "Design of PET-Detector with improved characteristics" Preprint INR RAS 1271/2016.

